Two-line Josephson traveling wave parametric amplifier

Victor K. Kornev, Alena N. Nikolaeva, and Nikolay V. Kolotinskiy*
Lomonosov Moscow State University, Moscow, Russia

Feasibility of two-line design of Josephson traveling wave parametric amplifier aimed at increase of the allowed pump wave energy and hence the gain growth is analyzed and discussed. Serious restrictions follow from both the cyclic energy transfer of the pump, signal and idler waves in the coupled waveguide lines and the phase mismatch of the waves. Besides, impact of the artificial line discreteness on the phase mismatch is considered as well.

Keywords: JTWPA, parametric amplification, traveling-wave amplifiers, Josephson junctions

I. INTRODUCTION

The parametric amplification mechanism enables extremely high-sensitive amplifiers capable of providing a noise temperature T_N lower than the ambient temperature. A traveling wave design concept of the amplifiers allows overcoming a gain-bandwidth trade-off that is peculiar to cavity-based parametric amplifiers. Josephson traveling wave parametric amplifiers (JTWPAs) are based on the use of artificial discrete lines composed of Josephson-junction cells which can consist of either single Josephson junctions or SQUIDs of different types (with different numbers of junctions). These amplifiers capable of working at low and very low temperatures and approaching a quantum limit level sensitivity are considered as promising readout devices in the field of precision quantum measurements, quantum communications and quantum computing (see [1, 2], and review [3]). In the capacity of the working reactive parameter, JTWPAs exploit a strongly nonlinear kinetic inductance of Josephson junctions

$$L_J = L_{J0}/\cos(\varphi) \tag{1}$$

attributable to their superconducting current component

$$I_s = I_c \sin(\varphi), \tag{2}$$

where I_c is the critical current of Josephson junction, φ is the Josephson-junction phase, $L_{J0} = \Phi_0/(2\pi I_c)$, and $\Phi_0 = h/(2e)$ is the magnetic flux quantum.

In JTWPA, the energy of the pump wave is used up in its transfer to both the signal and idle waves, as well as to the higher harmonics and undesired components with combined frequencies. This means that both the achievable gain and dynamic range are restricted by the depletion of the pump wave [4, 5], as the starting amplitude of the pump wave is limited by the critical current values of the Josephson junctions used. A two-line JTWPA design driven by magnetic flux has been proposed [6] for the purpose of problem solving. In this design, a distinct non-Josephson (linear) transmission line is used for pump wave's propagation. The pump wave, with a sufficiently high amplitude, applies traveling magnetic flux to the SQUID-like cells in the signal line to provide the modulation of the cells' inductances in a traveling wave pattern [7]. However,

from our point of view, one needs more fundamental consideration of the two-line amplifier designs, especially since no successfully realizations of such JTWPAs has been reported so far.

II. CONSIDERATION OF TWO COUPLED WAVEGUIDES

In this paper, we analyse and discuss the feasibility of JTWPAs based on using two coupled artificial waveguide lines, taking into consideration also the discreteness of the lines.

Figure 1 shows equivalent circuits of two coupled waveguide lines with capacitive (a) and inductive (b) couplings realised through either the linking capacitance C_0 or the mutual inductance M, respectively. In the continuum approximation, the telegraph equations for the first system can be written as follows:

$$\frac{\partial U_1}{\partial x} = -L_1 \frac{\partial I_1}{\partial t}, \tag{3}$$

$$\frac{\partial I_1}{\partial x} = -C_1 \frac{\partial U_1}{\partial t} - C_0 \frac{\partial(U_1 - U_2)}{\partial t}, \tag{4}$$

$$\frac{\partial U_2}{\partial x} = -L_2 \frac{\partial I_2}{\partial t}, \tag{5}$$

$$\frac{\partial I_1}{\partial x} = -C_2 \frac{\partial U_2}{\partial t} - C_0 \frac{\partial(U_2 - U_1)}{\partial t}, \tag{6}$$

where $U_{1,2}$ and $I_{1,2}$ are the voltage and the current in the lines 1 and 2, respectively. These equations yield in the following set of two coupled wave equations:

$$v_{01}^2 \frac{\partial^2 U_1}{\partial x^2} = \frac{\partial^2 U_1}{\partial t^2} - \alpha_1 \frac{\partial^2 U_2}{\partial t^2}, \tag{7}$$

$$v_{02}^2 \frac{\partial^2 U_2}{\partial x^2} = \frac{\partial^2 U_2}{\partial t^2} - \alpha_2 \frac{\partial^2 U_1}{\partial t^2}, \tag{8}$$

where $v_{01}^2 = (L_1 C_1)^{-1}$, $v_{02}^2 = (L_2 C_2)^{-1}$ are the partial phase velocities in square, $\alpha_1 = C_0/(C_1 + C_0) \approx C_0/C_1$, $\alpha_2 = C_0/(C_2 + C_0) \approx C_0/C_2$ are the capacitive coupling factors of the lines. In case of inductive coupling, telegraph equations
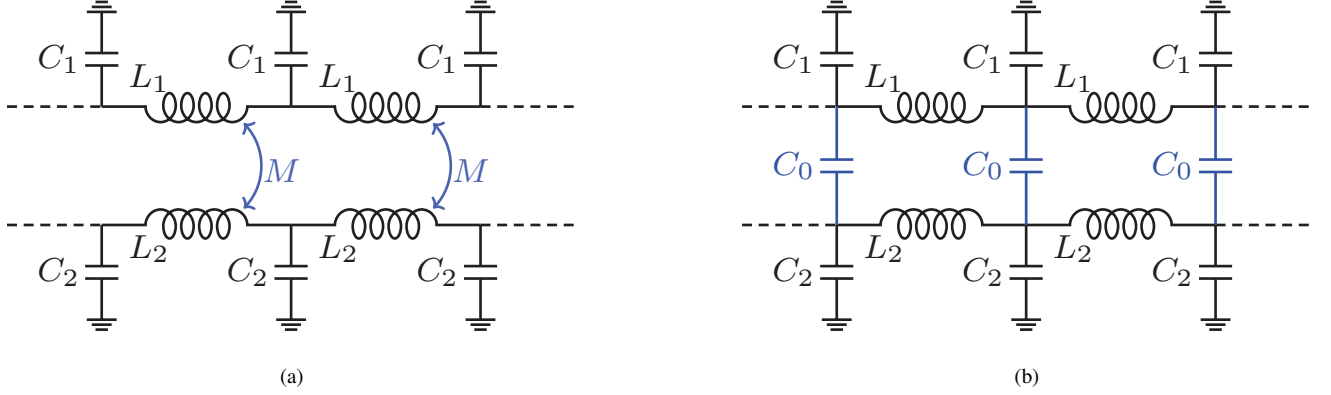
FIG. 1: Equivalent circuits of two coupled waveguide lines with capacitive (a) and inductive (b) couplings realized through either the linking capacitance C_0 or the mutual inductance M, respectively.

are as follows:

$$\frac{\partial U_1}{\partial x} = -L_1\frac{\partial I_1}{\partial t} - M\frac{\partial I_2}{\partial t}, \tag{9}$$

$$\frac{\partial I_1}{\partial x} = -C_1\frac{\partial U_1}{\partial t}, \tag{10}$$

$$\frac{\partial U_2}{\partial x} = -L_2\frac{\partial I_2}{\partial t} - M\frac{\partial I_1}{\partial t}, \tag{11}$$

$$\frac{\partial I_1}{\partial x} = -C_2\frac{\partial U_2}{\partial t}, \tag{12}$$

and yield in the similar set of two coupled wave equations:

$$v_{01}^2\frac{\partial^2 I_1}{\partial x^2} = \frac{\partial^2 I_1}{\partial t^2} - \eta_1\frac{\partial^2 I_2}{\partial t^2}, \tag{13}$$

$$v_{02}^2\frac{\partial^2 I_2}{\partial x^2} = \frac{\partial^2 I_2}{\partial t^2} - \eta_2\frac{\partial^2 I_1}{\partial t^2} \tag{14}$$

where $v_{01}^2 = (L_1C_1)^{-1}$, $v_{02}^2 = (L_2C_2)^{-1}$ are the partial phase velocities in square, $\eta_1 = M/L_1$, $\eta_2 = M/L_2$ are inductive coupling factors of the lines.

Owing to the similarity of the wave equation sets (7), (8) and (13), (14), one can consider the only first one and looking for its solution as

$$U_1 = A\cos(\omega t - kx), \quad U_2 = B\cos(\omega t - kx). \tag{15}$$

In this case, Eqs. (7) and (8) give the following set of two linear equations for the wave amplitudes:

$$\left(k^2 v_{01}^2 - \omega^2\right)A + \alpha_1\omega^2 B = 0, \tag{16}$$

$$\alpha_2\omega^2 A + \left(k^2 v_{02}^2 - \omega^2\right)B = 0. \tag{17}$$

Equating determinant of the set to zero, one comes to the following equation

$$\left(k^2 v_{01}^2 - \omega^2\right)\left(k^2 v_{02}^2 - \omega^2\right) - \alpha_1\alpha_2\omega^4 = 0. \tag{18}$$

Solution of this equation gives two values for the squared wave vector k^2 and hence two values for the squared phase velocity $v^2 = \omega^2/k^2$.

In the case of identical lines, when $v_{01}^2 = v_{02}^2 = v_0^2$ and $\alpha_1 = \alpha_2 = \alpha$, the equation solution is as follows:

$$k^2 = \frac{\omega^2}{v_0^2}(1\pm\alpha), \tag{19}$$

$$v^2 = \frac{v_0^2}{(1\pm\alpha)} \approx v_0^2(1\mp\alpha), \tag{20}$$

$$k_{1,2} = \frac{\omega}{v_0}\left(1\pm\frac{\alpha}{2}\right) = k_0\pm\Delta k, \tag{21}$$

$$v_{1,2} = \frac{v_0}{(1\pm\frac{\alpha}{2})} \approx v_0\left(1\mp\frac{\alpha}{2}\right) = v_0\mp\Delta v, \tag{22}$$

where $k_0 = \omega/v_0$, $\Delta k = (a/2)k_0$, and $\Delta v = (a/2)v_0$.

Thus, the wave process in both lines consists of two waves having different phase velocities. Amplitude ratio can be easily obtained from Eqs. (16) and (17):

$$\chi_{1,2} \equiv \left.\frac{B}{A}\right|_{k_{1,2}} = \frac{\alpha\omega^2}{\left(k^2 v_0^2 - \omega^2\right)} = \frac{\alpha}{(1\pm\alpha) - 1} = \pm 1. \tag{23}$$

And therefore, the wave process in the lines is as follows:

$$U_1 = A_1\cos(\omega t - k_1 x) + A_2\cos(\omega t - k_2 x), \tag{24}$$

$$U_2 = A_1\cos(\omega t - k_1 x) - A_2\cos(\omega t - k_2 x). \tag{25}$$

When rf signal source $U = A\cos(\omega t)$ is applied to input of the only one of the two lines, $e.g.$ to the first line, it corresponds to the following simple boundary conditions

$$A_1 + A_2 = A, \quad A_1 - A_2 = 0, \tag{26}$$

resulting in amplitude values

$$A_1 = -A_2 = A/2. \tag{27}$$

and hence in the following wave dynamics:

$$U_1 = A\cdot\cos\left(\frac{k_1 - k_2}{2}x\right)\cos\left(\omega t - \frac{k_1 + k_2}{2}x\right)$$
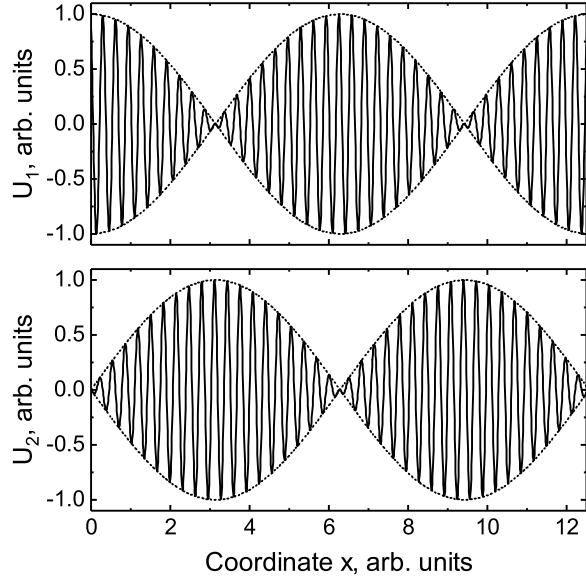$$= A\cdot cos(\alpha k_0 x)\cos(\omega t - k_0 x), \tag{28}$$

FIG. 2: Beat wave process in two coupled identical waveguide lines, when rf signal source $U = A\cos(\omega t)$ is connected to input of the only first line.

$$U_2 = A \cdot \sin\left(\frac{k_1 - k_2}{2}x\right)\sin\left(\omega t - \frac{k_1 + k_2}{2}x\right)$$
$$= A \cdot \sin(\alpha k_0 x)\sin(\omega t - k_0 x). \quad (29)$$

This is a beat process corresponding periodical transfer of the wave energy from one waveguide line to the other line and back as shown in Fig. 2. Any coupling of identical waveguide lines leads to strong their connectedness yielding in full energy transferring between the lines, and values of the coupling factors α_1, α_2 influence only on the periodic beat length

$$\Lambda = 2\pi/(k_1 - k_2) \quad (30)$$

In the case of nonidentical waveguide lines having different partial phase velocities and coupling factors, the solution of Eq. (18) has a much more complicated form. However, at weak connectedness of the lines, when

$$4\alpha_1\alpha_2\frac{v_{01}^2 v_{02}^2}{\left|v_{02}^2 - v_{01}^2\right|^2} \ll 1, \quad (31)$$

the solution can be expressed approximately as follows (as-

suming that $v_{02}^2 > v_{01}^2$):

$$k_1^2 = \frac{\omega^2}{v_{01}^2}\left[1 + \frac{\alpha_1\alpha_2 v_{01}^2}{\left(v_{02}^2 - v_{01}^2\right)}\right] = k_{01} + \Delta k_1, \quad (32)$$

$$k_2^2 = \frac{\omega^2}{v_{02}^2}\left[1 - \frac{\alpha_1\alpha_2 v_{02}^2}{\left(v_{02}^2 - v_{01}^2\right)}\right] - k_{02} + \Delta k_2, \quad (33)$$

$$v_1^2 = v_{01}^2\left[1 - \frac{\alpha_1\alpha_2 v_{01}^2}{\left(v_{02}^2 - v_{01}^2\right)}\right] = v_{01} + \Delta v_1, \quad (34)$$

$$v_2^2 = v_{02}^2\left[1 + \frac{\alpha_1\alpha_2 v_{02}^2}{\left(v_{02}^2 - v_{01}^2\right)}\right] = v_{02} + \Delta v_2, \quad (35)$$

where $k_{01} = \omega/v_{01}$, $k_{02} = \omega/v_{02}$,

$$\Delta k_1 = \frac{\alpha_1\alpha_2 v_{01}^2}{2\left(v_{02}^2 - v_{01}^2\right)}k_{01}, \quad (36)$$

$$\Delta k_2 = \frac{\alpha_1\alpha_2 v_{02}^2}{2\left(v_{02}^2 - v_{01}^2\right)}k_{02}, \quad (37)$$

and

$$\Delta v_1 = \frac{\alpha_1\alpha_2 v_{01}^2}{2\left(v_{02}^2 - v_{01}^2\right)}v_{01}, \quad (38)$$

$$\Delta v_2 = \frac{\alpha_1\alpha_2 v_{02}^2}{2\left(v_{02}^2 - v_{01}^2\right)}v_{02}. \quad (39)$$

In this case, amplitude ratio is different:

$$\chi_1 \equiv \left.\frac{B}{A}\right|_{k_1} = -\frac{\alpha_2 v_{01}^2}{\left(v_{02}^2 - v_{01}^2\right)} \approx -\frac{\alpha_2 v_{01}}{2\left(v_{02} - v_{01}\right)}, \quad (40)$$

$$\chi_2 \equiv \left.\frac{B}{A}\right|_{k_2} = \frac{\left(v_{02}^2 - v_{01}^2\right)}{\alpha_2 v_{01}^2} \approx -\frac{1}{\chi_1}. \quad (41)$$

In force of weak connectedness, coefficient $|\chi_1|$ is small, while $|\chi_2|$ is oppositely high.

When rf signal source $U = A\cos(\omega t)$ is applied to input of the only first line, boundary conditions

$$A_1 + A_2 = A, \quad \chi_1 A_1 + \chi_2 A_2 = 0 \quad (42)$$

yield in

$$A_1 = \frac{\chi_2}{(\chi_2 - \chi_1)}A, \quad A_2 = -\frac{\chi_1}{(\chi_2 - \chi_1)}A. \quad (43)$$

Thus, the wave process in the coupled nonidentical lines can be written as follows:

$$U_1 = A_1\cos(\omega t - k_1 x) + A_2\cos(\omega t - k_2 x)$$
$$= D(x)\cos(\omega t - k_1 x + \theta(x)), \quad (44)$$

$$U_2 = A_1\cos(\omega t - k_1 x) - A_2\cos(\omega t - k_2 x)$$
$$= 2A\frac{|\chi_1|\chi_2}{(\chi_2 - \chi_1)}\sin\left(\frac{(k_1 - k_2)}{2}x\right)$$
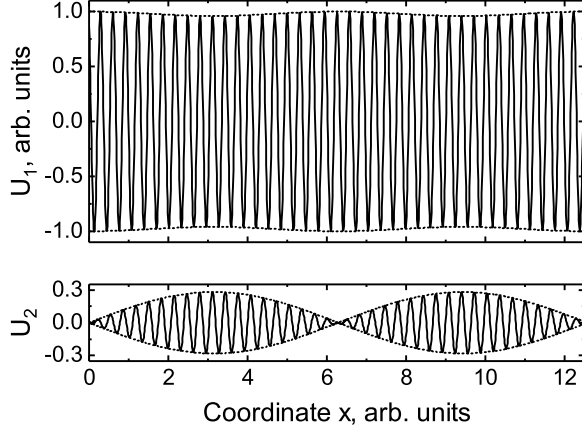$$\times \sin\left(\omega t - \frac{(k_1 + k_2)}{2}x\right), \quad (45)$$

FIG. 3: Beat wave process in two coupled nonidentical waveguide lines at weak connectedness of the lines, when rf signal source $U = A\cos(\omega t)$ is connected to input of the only first line.

FIG. 4: Fragment of two artificial waveguide lines of the flux driven JTWPA [6]. In the design, the pump wave current I_p flowing through the inductance L of the first line applies magnetic flux to the dc SQUID cell of the second (signal) line and provides periodic modulation of the cell inductance.

where

$$D(x) = A_1 \sqrt{1 + 2\cos\left(\frac{k_1 - k_2}{2}x\right)\frac{A_2}{A_1} + \left(\frac{A_2}{A_1}\right)^2}, \quad (46)$$

$$\tan(\theta) = \frac{A_2 \sin\left(\frac{k_1 - k_2}{2}x\right)}{A_1 + A_2 \cos\left(\frac{k_1 - k_2}{2}x\right)} \approx \frac{A_2}{A_1}\sin\left(\frac{k_1 - k_2}{2}x\right). \quad (47)$$

This is also beat-like process with the cycle length (30) but with much lower energy transferring from the first line to the second one and back due to weak connectedness as shown in Fig. 3.

III.   TWO-LINE JTWPA CRITICAL ISSUES

In the case of the two-line JTWPA, the wave processes shown in Figs. 2 and 3 for strong and weak connectedness of the lines are described as the pump wave propagation, as well as the signal and idler waves propagation. One can suppose that the pump signal is applied to the input of the first line while the input signal is applied to the second line. Then, the pump wave penetrates into the second line in the form of beats and changes phase by π every beat cycle. This fact limits the possible length of the used lines to the only one beat cycle length Λ (described by Eq. (30)) or even less. Indeed, at strong connectedness, the length of the coupled lines should be appreciably less than the beat cycle length since the permissible amplitude of the pump wave propagating in the second line is restricted by the critical current value of Josephson junctions. This limitation of the line length imposes a restriction on the attainable gain of the JTWPA. Moreover, the inevitable leak of the signal and idler waves into the other line additionally decreases the gain.
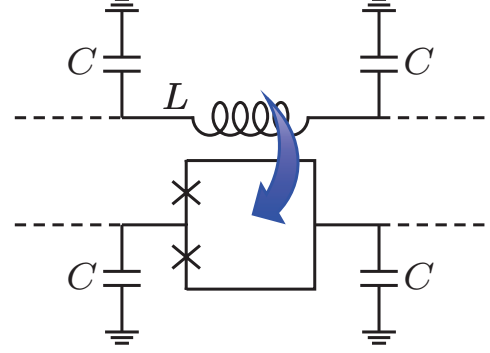
All these restrictions are actual also for the flux driven JTWPA [6] based on using two magnetically coupled artificial lines, where one of the lines is composed of dc SQUID cells as shown in Fig. 4. To apply some flux to the SQUID cells by a pump wave propagating along the other line to modulate the cell inductance, some mutual inductance value M has to be provided between the inductance L of the first line (used for pump wave) and half an inductance $L_{SQ}/2$ of the SQUID loop. In this case, the pump wave current I_p flowing through the inductance L induces also electromotive difference across the SQUID cell

$$U = -\frac{M}{2} \cdot \frac{dI_p}{dt} = -i\omega_p \frac{M}{2} I_p. \quad (48)$$

This fact evidences the existence of mutual coupling of the lines characterized by coupling factor $\eta = M/(2L)$. In such a way, the flux driving process will be accompanied by a transfer of the pump wave energy into the second (signal) line as well as also by a leak of the signal and idler waves into the other line.

The other important drawback and restrictions follow from the presence of an inevitable phase mismatch between the pump wave and the signal and idler waves in the most interesting case of a weak connectedness of the coupled lines. As seen from expressions Eqs. (32) and (33), in continuum approximation the signal and the idler waves propagating in the same waveguide line have the same phase velocity equal to either v_1 or v_2 (in dependence of the number of the used line). However, the pump signal transferred from the other line propagates along this line with other phase velocity $\bar{v}$ corresponding to the mean wave vector $(k_{01} + k_{02})/2$ as shown in Fig. 5.

Artificial discrete LC waveguide lines should be descried by discrete telegraph equations:

$$I_n - I_{n+1} = i\omega C U_n, \quad (49)$$
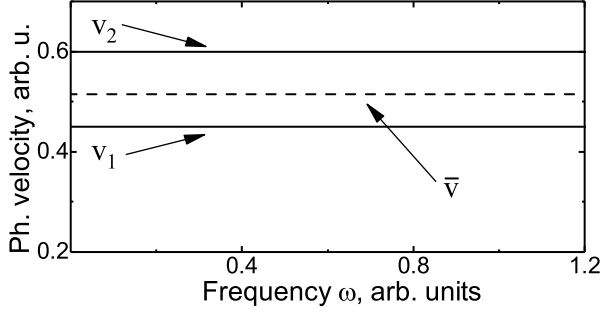
$$U_n - U_{n-1} = i\omega L I_{n+1}, \quad (50)$$

FIG. 5: Phase velocities v_1 and v_2 (solid lines) of the two eigen waves in the system of two coupled continuum waveguide lines at weak connectedness. Dashed line shows phase velocity $\bar{v}$ corresponding to the mean wave vector $(k_1 + k_2)/2$
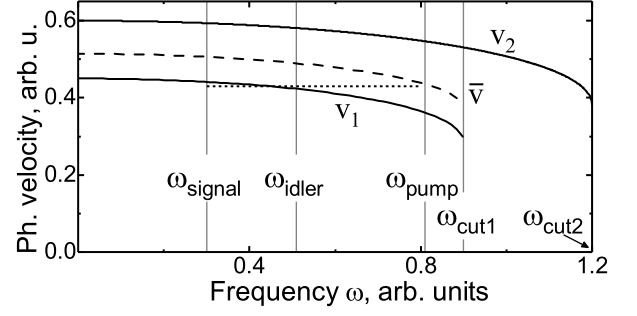
.

FIG. 6: Phase velocities v_1 and v_2 (solid lines) of the two eigen waves in the system of two coupled discrete waveguide lines with different cut-off frequencies at weak connectedness. Dashed line shows phase velocity $\bar{v}$ corresponding to the mean wave vector $(k_1 + k_2)/2$.

where the propagating wave is considered as a harmonic wave, and the cell size of the discrete line $a = 1$. These equations result in the following dispersion expression:

$$\sin^2(k/2) = \frac{\omega^2}{\omega_{cut}^2} \quad (51)$$

and the phase velocity

$$v = \frac{\omega}{k} = \frac{\omega}{2\,arcsin\left(\frac{\omega}{\omega_{cut}}\right)}, \quad (52)$$

where

$$\omega_{cut} = \frac{2}{\sqrt{LC}} \quad (53)$$

is the cut-off frequency of the discrete line. Moreover, such a discrete line has complex wave impedance

$$Z_0 = i\omega L/2 + \sqrt{L/C - (\omega L)^2/4} = \sqrt{L/C}\cdot e^{i\theta} \quad (54)$$

where

$$\theta = arcsin\left(\frac{\omega}{\omega_{cut}}\right). \quad (55)$$

The existence of the cut-off frequency gives good possibility to keep the higher harmonics of pump signal and the intermodulation components out of the frequency band. However, in a one-line JTWPA, the frequency dependent phase velocity does not allow achieving good phase matching between the pump, signal and idler waves and hence a higher gain in wide frequency band without an additional dispersion engineering technique. The restrictions can be mitigated in the one-line JTWPA with using 4-wave mode of operation: $\omega_s + \omega_i = 2\omega_p$, when all the waves frequencies are located nearer with each other in the vicinity of $\omega_{cut}/3$ where the wave velocities are quite close, and at the same time, both the harmonics of ω_p and the intermodulation components produced by the cubic nonlinearity are above the cut-off frequency.

In the case of a two-line JTWPA, one can recommend to use per contra 3-wave mode of operation $\omega_s + \omega_i = \omega_p$ as a better trade-off. Figure 6 shows the phase velocities v_1 and v_2 of the two eigen waves in the system of two coupled discrete waveguide lines with different cut-off frequencies at weak connectedness, as well as a possible frequency scheme corresponding to the 3-wave operation mode, where the pump source is connected to the line 2 and the pump wave propagates along the line with phase velocity v_2. The signal source is connected to input of the line 1 and the signal wave propagates along this line with phase velocity v_1 together with idler wave. The pump wave penetrates in part into the line 1 and then propagates along the line with the phase velocity $\bar{v}$ (shown by dashed line) corresponding to the mean wave vector $(k_1 + k_2)/2$. In the shown frequency scheme, this velocity is quite close to the one of the signal and idler waves. This allows achieving quite well phase matching needed for the effective signal amplification.

IV. CONCLUSION

In such a way, the two-line design of Josephson traveling wave parametric amplifier meets with serious restrictions following from both the cyclic energy transfer of the travelling waves in the coupled waveguide lines and the phase mismatch of the pump, signal and idler waves due to the line coupling and the line discreteness.

CREDIT AUTHORSHIP CONTRIBUTION STATEMENT

V.K.K.: conceptualization (lead), formal analysis (lead), investigation (equal), methodology (lead), project administra-

tion (supporting), supervision (lead), validation (lead), writing – original draft (lead), writing – review & editing (equal); **A.N.N.**: conceptualization (supporting), formal analysis (supporting), investigation (equal), methodology (supporting), visualization (supporting); **N.V.K.**: conceptualization (supporting), funding acquisition (lead), investigation (equal), project administration (lead), software (lead), supervision (supporting), validation (supporting), writing – review & editing (equal).

CONFLICT OF INTEREST STATEMENT

The authors declare no conflict of interest. The funder had no role in any part of the manuscript preparation process.

DATA AVAILABILITY STATEMENT

The data that support the findings of this study are available from the corresponding author upon reasonable request.

[1] C. Macklin, K. O'Brien, D. Hover, M. E. Schwartz, V. Bolkhovsky, X. Zhang, W. D. Oliver, and I. Siddiqi. A near–quantum-limited josephson traveling-wave parametric amplifier. *Science*, 350(6258):307–310, October 2015. `doi:10.1126/science.aaa8525`.

[2] Michael Haider, Johannes A. Russer, Jesus Abundis Patino, Christian Jirauschek, and Peter Russer. A josephson traveling wave parametric amplifier for quantum coherent signal processing. In *2019 IEEE MTT-S International Microwave Symposium (IMS)*. IEEE, June 2019. `doi:10.1109/mwsym.2019.8700875`.

[3] Martina Esposito, Arpit Ranadive, Luca Planat, and Nicolas Roch. Perspective on traveling wave microwave parametric amplifiers. *Applied Physics Letters*, 119(12):120501, 2021. `doi:10.1063/5.0064892`.

[4] A. B. Zorin. Josephson traveling-wave parametric amplifier with three-wave mixing. *Physical Review Applied*, 6(3):034006, September 2016. `doi:10.1103/physrevapplied.6.034006`.

[5] A. B. Zorin, M. Khabipov, J. Dietel, and R. Dolata. Traveling-wave parametric amplifier based on three-wave mixing in a josephson metamaterial. In *2017 16th International Superconductive Electronics Conference (ISEC)*. IEEE, June 2017. `doi:10.1109/isec.2017.8314196`.

[6] A.B. Zorin. Flux-driven josephson traveling-wave parametric amplifier. *Physical Review Applied*, 12(4):044051, October 2019. `doi:10.1103/physrevapplied.12.044051`.

[7] Alena N. Nikolaeva, Victor K. Kornev, and Nikolay V. Kolotinskiy. Bi-squid versus dc squid in flux-driven traveling-wave parametric amplifier. *Applied Sciences*, 13(14):8236, July 2023. `doi:10.3390/app13148236`.